Carbon-Tolerant Ni/ScCeSZ Via Aqueous Tape Casting for IT- SOFCs

Arifin, Nor; Button, Timothy; Steinberger-Wilckens, Robert

Carbon-Tolerant Ni/ScCeSZ Via Aqueous Tape Casting for IT- SOFCs

N.A.Arifin[a], T.W.Button [b], R.Steinberger-Wilckens [a],

[a] School of Chemical Engineering, University of Birmingham, Edgbaston, Birmingham B15 2TT, UK
[b] School of Metallurgy and Materials, University of Birmingham, Edgbaston, Birmingham B15 2TT, UK

Nickel-Yttria stabilized zirconia (Ni/8YSZ) and Nickel Ceria doped-Scandia stabilised zirconia (Ni/10ScCeSZ) anode supported cells were successfully fabricated using a reverse aqueous tape casting method. The performance of the full cells were tested using both hydrogen and dry biogas at the anode side and ambient air at the cathode side in the temperature range 750°C to 800°C. In hydrogen, Ni/10ScCeSZ showed better performance at 800°C compared to the Ni/8YSZ cell. Switching the fuel from hydrogen to dry biogas, the performance of the Ni/8YSZ cell reduced significantly from 0.31 W/cm^2 to 0.06 W/cm^2. With Ni/10ScCeSZ cells, the cell performance in biogas was 4 times higher than the corresponding Ni8YSZ cells. The maximum power density decreased only from 0.36 W/cm^2 to 0.22 W/cm^2 in Ni/10ScCeSZ cell tested when switched from hydrogen to biogas. The results of this work indicate the possibility of using biogas or other carbonaceous fuel in SOFCs without the addition of water (steam).

Introduction

Solid Oxide Fuel Cells (SOFCs) offer conversion of hydrogen or methane with high electrical efficiency. The fuel flexibility of SOFCs makes the technology more compelling compared to other fuel cells as it can operate with a range of other fuels than hydrogen. As abundant amounts of biogas are readily available from wastewater treatment from various sources, utilizing biogas directly as a fuel is highly desirable both in terms of the environment and cost.

Theoretically, direct utilization of any hydrocarbon as fuel for SOFCs is possible; however, this leads to carbon deposition and degrades the SOFC's anode. Biogas consists of methane, carbon dioxide, and trace of impurities. With direct use of biogas fuel, the possible reactions between methane and carbon dioxide that may take place are shown in Equations 1 and 2.

Carbon dioxide (dry) reforming(1, 2):

$$CH_4 + CO_2 \rightarrow 2H_2 + 2CO \quad [1]$$

Reverse water-gas shift reaction(1, 2):

$$CO_2 + H_2 \leftrightharpoons H_2O + CO \quad [2]$$

The possible reactions for carbon deposition are by methane cracking (Equation 3), the Boudouard reaction (Equation 4) and the reverse syn-gas reaction (Equation 5)(1, 2).

$$CH_4 \leftrightharpoons C + 2H_2 \quad [3]$$

$$2CO \leftrightharpoons C + CO_2 \quad [4]$$

$$H_2 + CO \leftrightharpoons C + H_2O \quad [5]$$

Carbon deposition will reduce the triple phase boundary (TPBs) length, resulting from deactivation of the nickel catalyst and inhibition of fuel diffusion in the anode. After some time, this will deactivate the entire fuel cell anode. Thus, in order to use carbonaceous fuel, new materials need to replace the benchmark anode material Nickel-Yttria Stabilised Zirconia (Ni/8YSZ).

Even though a lot of materials research has been undertaken to enable operation with biogas or other carbonaceous fuels, the development of alternative anode materials that can replicate high power performance at temperatures below 800°C with negligible carbon deposition at acceptable cost has not been achieved to date. Either the electronic conductivity is too low or the cost is too high when using precious metals. Despite the lack of attention given to Nickel-Ceria-doped Scandia stabilised Zirconia (Ni/ScCeSZ) cermets in the last decade, this matured material actually holds several advantages over the Ni/8YSZ and other alternative anode materials. It exhibits less carbon deposition, partly due to the 1 mol% ceria dopant, better tolerance to sulphur poisoning, and higher ionic conductivity (3, 4).

In planar SOFC mass manufacturing production, tape casting is the most suitable process as large numbers of cells can be produce in one batch. Currently solvent-based tape casting is used as high quality green tapes can be easily achieved. However, due to the highly flammable solvent which is toxic and hazardous both to humans and the environment, there is renewed interest in aqueous tape casting. With optimisation, high quality of green tapes can be achieved as demonstrated by several recent reports(5, 6).

In this paper, we report comparative study of using Ni/10ScCeSZ as a replacement for Ni/8YSZ anodes in SOFCs operating with biogas using in-house cells fabricated via multilayer aqueous tape casting.

Experimental

Materials

For each layer of the SOFC cells, different commercial powders are used as different requirements and materials are needed. The as-received commercial powders used for electrolytes is 8YSZ (TZ-8YS TOSOH) with particle size of 0.869 μm (d_{50}). For the anode substrate, the cermet consist of as-received coarse NiO with particle size of 6-10 μm (d_{50}) (High Purity Grade A, Novamet) and pre-calcined 8YSZ (TZ-8YS TOSOH) in a weight ratio of 65:35. The Finer NiO with particle size of 0.7μm (d_{50}) (Pi-Kem) and as-received 8YSZ powder (TZ-8YS TOSOH) were mixed with the same ratio for the anode functional layer. The electrolyte layer used the same as-received 8YSZ powder. For Ni10ScCeSZ cells, 10ScCeSZ (DKKK) with particle size of 0.511 μm (d_{50}) was used in all the layers instead of the 8YSZ. The cathode powder used was Lanthanum Strontium Manganite (PRAXAIR). Wire connectors used in the conductivity and cell performance tests were 99.99% silver.

Conductivity test

Commercial powder of 8YSZ (TZ-8YS TOSOH) and 10ScCeSZ (DKKK) were used in this test were dry-pressed at 30kPa using a 2.5cm diameter die and sintered at 1450°C. The sintered pellets were polished to emphasize the evenness of the surface. Conductivity tests utilised a four-probe method with silver metal wires attached using silver paste to the sample at four points where two opposite points were connected to a voltmeter and the other two points connected to the current supply. The current was set to 0.05A and corresponding voltages were recorded for temperatures ranging from 600 to 850°C in air.

Reverse Aqueous Tape casting

For the electrolyte slurry, a water-based emulsion binder system (WB4101) supplied by Polymer Innovations Inc. (USA) was used with the composition as shown in table 1. For both anode layers, first the cermet powders were mixed with distilled water, dispersant and anti-foaming agent by ball milling for 24 hours at 120 rpm for complete dispersion of the powders. A mixture of different sizes of grinding media were used to ensure uniform homogeneity. 3 wt% tapioca starch added to the anode substrate slurry as pore former. Then the plasticizers and binder were added followed by a further 4 hours of ball milling at 70 rpm. Prior to ball milling, the PVA solution was prepared using distilled water with the weight ratio of 1:4 to ensure complete solubility of the solid PVA.

A long de-gassing process of up to 12 hours was employed to eliminate all bubbles, followed by 1-2 hours of slow rolling. The organics and optimum compositions for the anode substrate (AS) and anode functional layer (AFL) are shown in table 2. The solids loading used was 55 wt% (35 vol %), the amount of organics was 15.1 wt%, with water as solvent at 29.9 wt%. The binder-to-plasticiser ratio was 1:1. The amount of dispersant was determined by sedimentation tests and zeta potential values measured in previous work(6). The slurries were tape cast onto Mylar carrier film using a single blade laboratory tape casting machine with vacuum bed (L800 by MTI). The blade's gap height and speed were adjusted for each layer accordingly. A thin electrolyte layer was tape cast first with gap height of 0.10mm, followed by the AFL layer with gap height of 0.15mm

and finally the thick anode substrate layer with gap height of 2.00 mm. This method was adapted from Schaufbauer et al, 2004 (7) and Wang et al, 201 (8). Each layer was dried in in an oven before tape casting another layer on top of it. The drying temperature used was 70°C for the electrolyte and AFL, and 33°C for the thick anode substrate layer.

Button cells (3 cm diameter) produced using a metal punch cutter and co-sintered at 1350°C for Ni/8YSZ and 1280°C for Ni/10ScCeSZ for 4 hours with 1°C heating rate and organic burnout stage at 550°C. The sintering temperature was the optimized temperature between the densification of electrolyte and cell flatness. Lanthanum Strontium Manganese (LSM) cathode ink were prepared by mixing the powder with ink vehicle (Haraeus V-737) using three-roll mill machine (BUHLER). The sintered half-cells were then hand painted with a 15µm thickness of LSM layer with an effective area of $2cm^2$ and sintered again at 1100°C. Full cell preparation is summarised in Figure 1.

TABLE 1: Tape Casting Composition (Electrolyte)

Chemicals	Function	Wt%
8YSZ/10ScCeSZ	Ionic phase	49.8
WB4101	Binder	19.3
DS001	Dispersant	2.0
DF002	Anti-foam	0.4
PL005	Plasticiser	0.5

TABLE 2: Tape Casting Composition (Anode layers)

Chemicals	Function	Wt %	
		AFL	AS
Nickel Oxide	Electronic phase	35.80	35.80
8YSZ/10ScCeSZ	Ionic phase	19.30	19.30
Tapioca Starch	Pore former	-	3.00
BASF Dispex Ultra 4404®	Dispersant	1.00	1.00
Water	Solvent	35.40	29.90
Antifoam 204	Antifoam	0.20	0.20
PVA	Binder	4.10	5.40
PEG 200	Plasticiser I	2.70	2.70
Glycerol	Plasticiser II	1.40	2.70

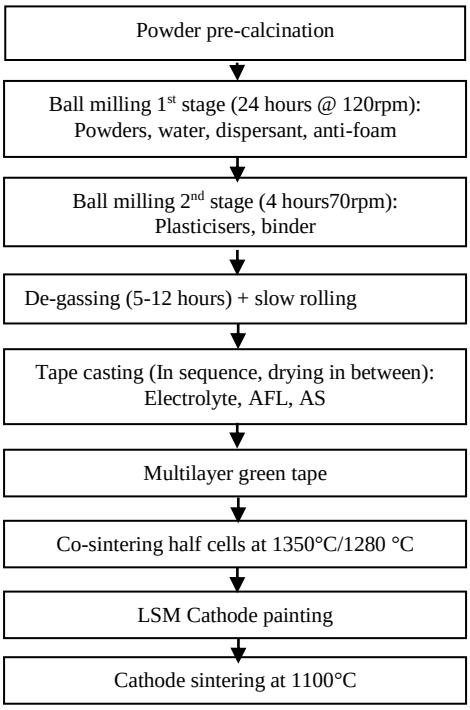

Figure 1: Full cell fabrication process used in this work

Cell Performance

Individual cells were mounted using dense silver paste on a 50 x 3 cm diameter alumina tube with fuel fed to the anode-side and the cathode side exposed to ambient air. Dense silver paste and silver wires were used to connect the cells to a Solartron Analytical (Model No 1400A) for performance and impedance measurements.

A range of test setups were used. Setup A used a flowrate of 60 mL/min of hydrogen (H_2) at two different temperatures, 750°C and 800°C. Setup B used a flowrate of 21 mL/min of hydrogen and 7 mL/min of helium (He). In Setup C 21mL/min of simulated biogas was used (comprising of 14 mL of methane (CH_4) and 7 mL/min of carbon

dioxide (CO_2)), and 7 mL/min of He. In setups B and C, a lower hydrogen flowrate (21 mL/min) and additional helium (7 mL/min) were also used in order to compare the results with previous work (2). In this work, helium was used since the outlet gasses were connected to a mass-spectroscopy for evaluation.

Result and Discussion

Ionic conductivity

The results of the conductivity tests of the sintered electrolyte materials are shown in Figure 2, where it can be clearly seen that 10ScCeSZ has a higher conductivity than 8YSZ at all temperatures, as expected. At 750°C, the conductivities of 8YSZ and 10ScCeSz were 0.09 S/cm and 0.16 S/cm respectively. These values are similar to the bulk conductivities measured by Verbraeken, Cheung, Suard and Irvine (9). The ionic conductivity of materials depends on the powder synthesis method and the size of the particles (9, 10). Thus, for the same materials big ranges of conductivity are reported. For this conductivity test, commercial powders with similar sizes were used and thus comparison of the values is meaningful.

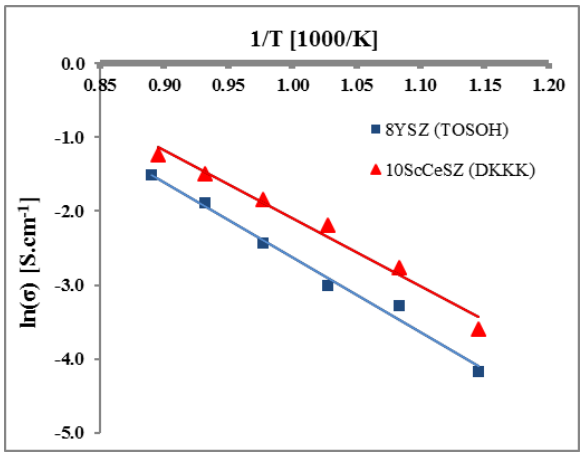

Figure 2. Ionic conductivity of sintered 8YSZ (TOSOH) vs 10ScCeSZ (DKKK) pellets.

Tape casting

Differences in the particle size characteristics and hence the surface area of the electrolyte powders affected the quality of the anode substrate green tapes. Using a tape casting formulation developed for NiYSZ resulted in cracks when NiScCeSZ was used, and a tape that was not flexible enough, as shown in Figure 3a. It was suspected that the drying rate inside the thick layer and on the top surface might be mismatched. Adding more glycerol (type II plasticizer) gave smooth and flexible tapes. Glycerol acts as Type II plasticizer that lowers the glass transition temperature, T_g (6), and has been widely used in aqueous tape casting processes. The composition in Table 2 is the final optimized composition used for both Ni/8YSZ and Ni/10ScCeSZ anode substrates. Figure 3b and 3c show multilayer green tapes consisting of electrolyte, anode functional layer, and anode substrate layer.

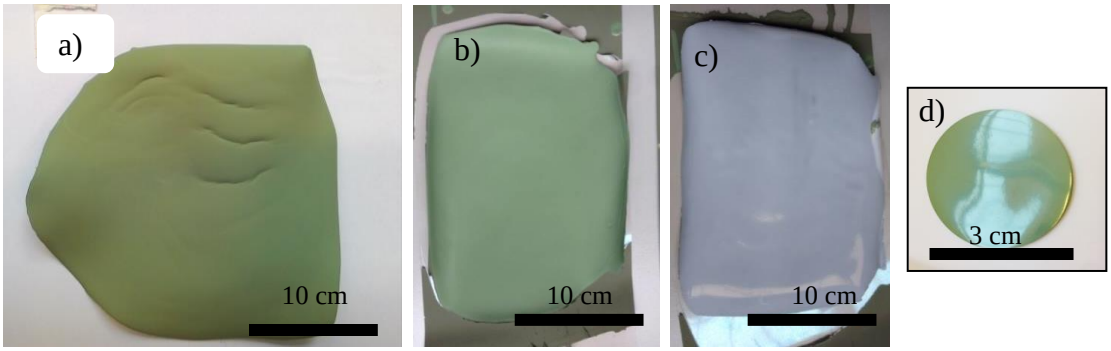

Figure 3: Dried green tape a) Cracked NiScCeSZ anode substrate layer, b) Multilayer green tape (anode side), c) Multilayer green tape (electrolyte side), d) Sintered half-cell.

Microstructure analysis

The SEM images in Figure 4a show that the SOFC desired layer characteristics - dense electrolyte and porous electrodes – have been achieved for both the yttria and scandia systems. Coarser nickel oxide and 3wt% of pore former were used in the thick anode substrate layer to ease gas diffusion; hence the porous, sponge-like structure. The sintered thickness of the electrolyte layer in the Ni/8YSZ cells was 10 to 12 µm while in the Ni/10ScCeSZ cells the thickness was 18 to 20 µm. The electrolyte layer for 10ScCeSZ was tape cast thicker due to one main reason: a performance test with an electrolyte thickness of 10 to 12 µm did not give an open circuit voltage (OCV) value of >1.0V. To achieve an acceptable OCV for the Ni/ScCeSZ cells, a thicker electrolyte layer was therefore chosen.

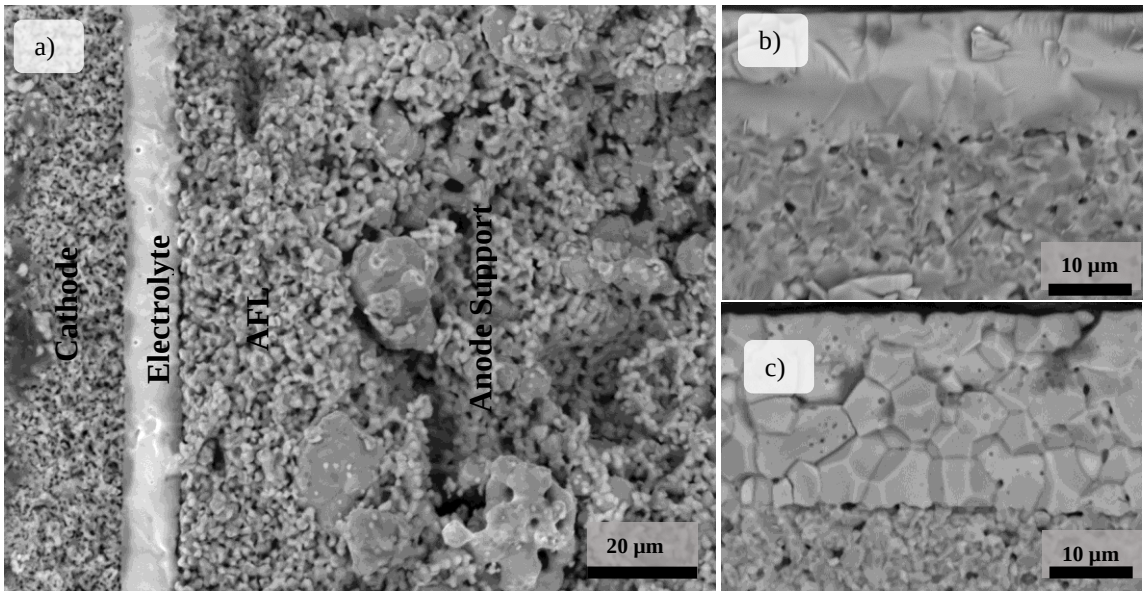

Figure 4: SEM microstructure of fracture surfaces of a) Ni8YSZ by reverse aqueous tape casting (cross-sectional), b) 8YSZ electrolyte layer, c) 10ScCeSZ electrolyte layer.

The structure of the electrolyte layer of these two materials was very different, as can be seen in Figures 4b and 4c. In the Ni/8YSZ cell (Fig 4(b)), the electrolyte layer shows no grain boundaries, while in the Ni/10ScCeSZ cell (Fig 4(c)) the grain boundaries

are clearly visible. As these images are from fracture surfaces it is assumed that the fracture modes in the YSZ and ScCeSZ layers are intragranular and intergranular respectively, indicating that the nature of the grain boundaries are different in the two systems. Grain boundaries can be a source of additional resistance, and this issue and the extra thickness of 10ScCeSZ electrolyte is suspected to affect the cell performance. Work is in progress to investigate these issues further.

Performance

Setup A. Using hydrogen at a high flow rate at 750°C, the maximum power density of both cells were almost the same, 0.37 W/cm^2 for the Ni/8YSZ cell and 0.39 W/cm^2 for the Ni/10ScCeSZ cell. At 800°C, the Ni10ScCeSZ cell showed approximately 19% better performance compared to the Ni/8YSZ cell, 0.63 W/cm^2 and 0.53 W/cm^2 respectively. Figure 5 presents the result for Setup A. The ohmic resistance of both of the cells at both temperatures were almost the same as shown in Table 3. Based on the conductivity tests and theory, Ni/10ScCeSZ should give better performance and lower ohmic resistance at lower temperature, but that was not the case in our work. The reason behind this are the thicker electrolyte layer that was necessary in order to get an acceptable OCV and possibly the different grain boundary properties in the 10ScCeSZ layer as discussed above.

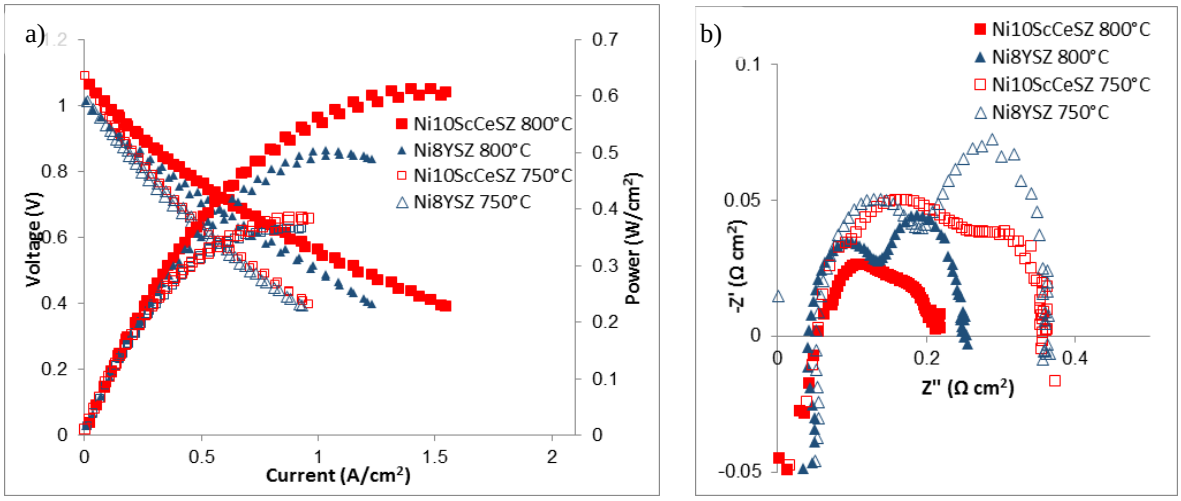

Figure 5: a) I-V curve of Ni/8YSZ vs Ni/10ScCeSZ cells tested in 60 mL/min hydrogen, b) Corresponding impedance of the Ni/8YSZ and Ni/10ScCeSZ cells.

Setup B and C. The differences in performance at 750°C using Setup B with a low hydrogen flow rate was more significant than at higher flow rate. With low flowrate, the maximum power density of the Ni/10ScCeSZ cell was 16% higher than the Ni/8YSZ cell; while in Setup A, it was only 5% higher. As illustrated in Figure 6; switching the fuel from hydrogen to biogas showed a dramatic reduction of the performance of the Ni/8YSZ cell. In biogas, the maximum power density was only 0.05 W/cm^2, compared to the initial value 0.31 W/cm^2 in hydrogen (84% performance drop). The OCV also dropped to 0.9V as illustrated in Figure 6. The same pattern of a dramatic drop in

performance of commercial Ni/8YSZ cells in biogas was observed previously by Troskialina, et al (2).

TABLE 3: Summary of performance tests with hydrogen and biogas

Cell Setup	Anode inlet	Material	Temp (°C)	Current at 0.7 V (A/cm^2)	Max Power Density (W/cm^2)	Ohmic Resistance (Ωcm^2)	Polarisation Resistance (Ωcm^2)
A	Hydrogen 60 mL/min H_2	Ni/8YSZ	750	0.39	0.37	0.05	0.31
			800	0.53	0.50	0.04	0.21
		Ni/10ScCeSZ	750	0.40	0.39	0.06	0.30
			800	0.63	0.61	0.05	0.16
B	Hydrogen 21 mL/min H_2 7 mL/min He	Ni/8YSZ	750	0.31	0.31	0.05	0.33
		Ni/10ScCeSZ	750	0.38	0.36	0.06	0.26
C	Biogas 14 mL/min CH_4 7 mL/min CO_2 7 mL/min He	Ni/8YSZ	750	0.06	0.05	0.05	0.95**
		Ni/10ScCeSZ	750	0.24	0.22	0.06	0.38

**approximated at lowest value

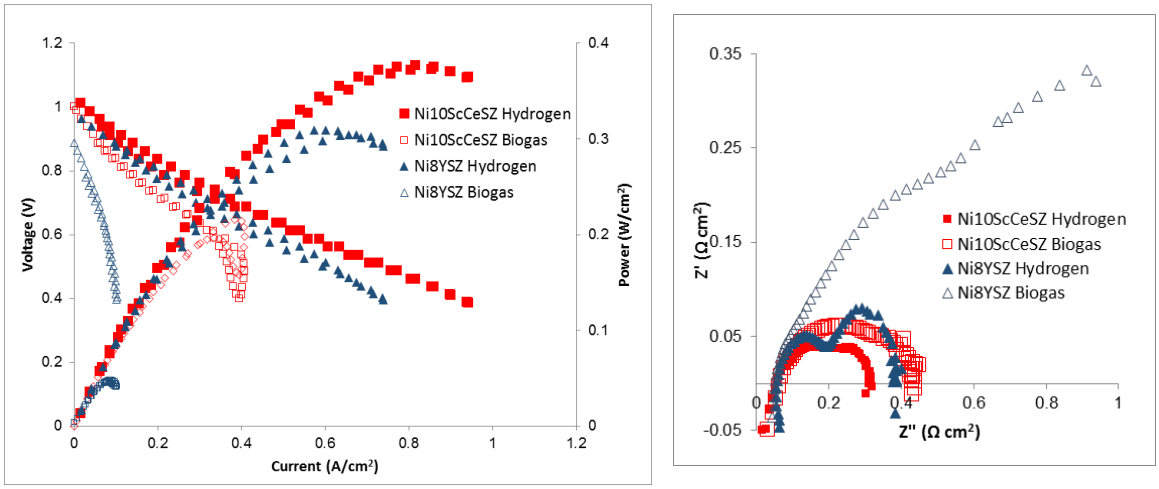

Figure 6: a) I-V curve of Ni/8YSZ vs Ni/10ScCeSZ cells tested in hydrogen and biogas (28mL/min), b) Impedance at 0.7V of Ni/8YSZ and Ni/10ScCeSZ cells.

It can be seen in the impedance plot in Figure 6 b) that the polarization resistance increases significantly for Ni/8YSZ with biogas but the ohmic resistance remains the same. This is interesting as in biogas, there is more fuel compared to hydrogen as the feed. In biogas, the syngas produces H_2 and CO by methane cracking as shown in equation 1.With the sudden drop of performance in Ni/8YSZ, it was suspected there was carbon build up on the anode (Equation 3-5), thus blocking the nickel surface which is the catalyst for the internal reforming of methane, and reducing efficiency of the reaction. This will be investigated further and the actual amount of carbon deposited on the anode surface will be quantified via Temperature Program Oxidation (TPO).

In contrast, when switched to biogas, the performance drop in the Ni/10ScCeSZ cell was only 39% (0.36 W/cm^2 to 0.22 W/cm^2). The OCV drop was insignificant and OCV remained above 1.0V. 1 mol% ceria is added as the third dopant in ScSZ to stabilize the cubic phase. Thus ScSZ powders are supplied commercially with 1mol% ceria in form of 10Sc1CeSZ. Ceria as a dopant has been proven to improve reforming, electrocatalytic performance, and resistance toward carbon deposition (1). Laycock et al (1) showed that ceria promotes the reaction between CO_2 and carbon through reactions (6) and (7) and promotes the reverse Boudouard reaction.

$$Ce_2O_3 + CO_2 \leftrightharpoons 2CeO_2 + CO \quad [6]$$

$$2CeO_2 + C \leftrightharpoons Ce_2O_3 + CO \quad [7]$$

The impedance in Figure 6(b) shows a 0.121Ωcm^2 increase when switched to biogas for the Ni/10ScCeSZ cell. For both cells, the increase in the polarization resistance agrees with the decrease of performance.

Conclusion

SOFC cells incorporating Ni/10ScCeSZ anodes and 10ScCeSZ electrolytes have been shown to perform better than Ni/8YSZ cermets and electrolytes both in hydrogen and in biogas. In hydrogen, the differences were more significant at lower flowrate at the same temperature. Switching to biogas led to a 84% reduction in performance in of Ni/8YSZ cells but only affected Ni/10ScCeSZ cells by 39%.

Acknowledgments

This work has been supported by the Council of Trust for the Bumiputera Malaysia (MARA) and Human Life Advancement Foundation (HLAF).

References

1. C. J. Laycock, J. Z. Staniforth and R. M. Ormerod, *Dalton Transactions*, **40**, 5494 (2011).
2. L. Troskialina. A. Dhir and R. Steinberger-Wiclkens, *ECS transaction* (2015).
3. M. R. Somalu, V. Yufit, D. Cumming, E. Lorente and N. P. Brandon, *International Journal of Hydrogen Energy*, **36**, 5557 (2011).
4. A. Hagen, J. F. B. Rasmussen and K. Thydén, *Journal of Power Sources*, **196**, 7271 (2011).
5. C. Fu, S. H. Chan, Q. Liu, X. Ge and G. Pasciak, *International Journal of Hydrogen Energy*, **35**, 301 (2010).
6. N. Arifin. T. Button. R. Steinberger-Wilckens, in *Proceedings of the 12th European SOFC Forum. 12. ed. European Fuel Cell Forum*, Lucerne (2016).
7. W. Schafbauer, N. H. Menzler and H. P. Buchkremer, *International Journal of Applied Ceramic Technology*, **11**, 125 (2014).
8. C. Wang, L. Luo, Y. Wu, B. Hou and L. Sun, *Materials Letters*, **65**, 2251 (2011).

9. M. C. Verbraeken, C. Cheung, E. Suard and J. T. S. Irvine, *Nat Mater*, **14**, 95 (2015).
10. J. Fergus, R. Hui, X. Li, D. P. Wilkinson and J. Zhang, *Solid Oxide Fuel Cells: Materials Properties and Performance*, CRC Press (2016).